

Research Article

Trajectory Planning in Complex Environments for Static and Moving Obstacles

Kalyanasundaram Madhu  ¹*¹Research Department, ZenToks, Dharmapuri, 635202, Tamilnadu, India.*Corresponding author: dr.kmadhu@zentoks.org**Article Info****Keywords:** Risk-bounded trajectory, Static Risk Contours, Dynamic Risk Contours, Autonomous vehicle, Moving Obstacle**Received:** 20.07.2025**Accepted:** 22.09.2025**Published:** 13.10.2025 © 2024 by the author's. The terms and conditions of the Creative Commons Attribution (CC BY) license apply to this open access article.**Abstract**

This paper presents a piecewise-linear approach for motion planning in uncertain environments punctured with static and moving obstacles. In such environments robots may encounter obstacles with unknown sizes, shapes, and locations. The probability of a robot colliding with an unknown obstacle entails a risk. The proposed approach offers a trajectory planning method that outputs a continuous-time optimal (shortest) trajectory that is guaranteed to have a bounded risk over the planning horizon. The optimal length of the path is determined by a moment optimization approach, and a hierarchy of semidefinite programs that yield increasingly finer lower bounds. In our method, we do not require any time discretization to handle continuous constraints. Using convex methods based on sum of squares (SOS) optimization, we produce continuous-time risk bounded trajectories without time discretization by solving the obtained non-convex time-varying optimization problem. The presented approach can be used for online trajectory planning problems, and it takes into account arbitrary probabilistic uncertainties and non-convex and nonlinear obstacles.

1. Introduction

Robots have to plan safe trajectories in the real world, that avoid static and moving obstacles, such as humans and vehicles, while taking into account the environment's uncertainties. Computationally difficult motion planning problems are known to exist in dynamic environments [1]. When planning in the presence of uncertainties and disturbances, safety is a major concern. As a result, uncertainty must be dealt with using robust and risk-aware approaches. The purpose of this paper is to analyze risk-bounded motion planning when robot perception is uncertain due to probabilistic uncertainties in the location, size, and geometry of obstacles. Rather than using an ordinary map with symbols of obstacles and open spaces, instead we use, we propose the construction of a risk map, called risk contours, which shows the risk information of different regions in the environment. In the presence of probabilistic uncertainties, risk is defined as the probability of robots colliding with obstacles. This type of mapping can be used to provide robots with trajectories to avoid risky areas and, generally, to plan motions with low risk. In risk-bounded motion planning, one aim to design trajectories whose probability of failure is limited by a predetermined value [2–4]. Probability distributions of uncertainties over nonconvex sets that describe the obstacle regions present a numerically difficult problem for risk computation in continuous space since it requires multivariate integrals. There are no closed form solutions for such integrals. To estimate the risk, one can use sampling-based methods as well as Boole's inequality, given obstacles and probabilities of uncertainties. Analytical bounds on the risk can only be determined by sampling methods, such as Monte Carlo techniques [5–7]. As a result, these approaches cannot be directly applied to risk bounded motion planning, which requires strict upper bounds on the risk [3]. Furthermore, Boole's inequality provides conservative upper bounds on the risk in the presence of linear convex obstacles. In [2, 4, 8], the solution to the problem of risk bounded motion planning in the presence of Gaussian distributions and convex obstacles is

based on Bole’s inequality. Risk-aware cost is calculated using Gaussian distributions and logistic functions by [9] to determine the distance between vehicles that is safe. [3] proposes a method to estimate risk in the presence of nonconvex regions that uses polynomial optimizations to compute upper and lower bounds on the probability of violating nonconvex safety constraints. In [10], the authors propose a method for modeling uncertain environments called risk contour maps, a method that has not been attempted before. In uncertain environments, risk contour maps are used to show information about risk in different regions. The notion of a Δ -risk contour enables us to construct such a map by representing points in the environment with a risk level that is less than or equal to the predefined risk level Δ . Maps showing risk contours are collections of such “ Δ -risk contours” with a range of risk levels Δ . Also, they noted, we cannot use direct risk estimation techniques such as Jasour et.al. described in [3] because first we need to discover risk contour in the environment along with their associated risk. In [11, 12], the authors develop convex optimizations based on the theory of moments and nonnegative polynomials for solving chance constrained optimizations. In this paper, we offer a systematic method for estimating risk contours in the presence of nonconvex obstacles and bounded probabilistic uncertainties. Convex optimizations are provided in the form of sum of squares (SOS) optimizations. In SOS optimization, we look for polynomials whose coefficients satisfy linear matrix inequalities. In the control and motion planning of robots and autonomous systems, SOS optimization is applicable in various ways, (e.g., see [3, 13–18]). The recent studies in [10, 12] on chance constrained optimization tackle SOS optimization leveraging the inner approximations of Δ -risk contours. Therein, the contours are parameterized by a single random variable following a uniform distribution. Building upon this result, we consider a more general scenario, where the risk contours are characterised by 2 independent variables that belong to different probability distributions. This allows to capture a more practical scenario where the uncertainties are non-uniform and stem from different sources. This rest of this paper is structured as follows: Polynomials, moments, and sum-of-squares optimization are defined in Section II, as well as the notation used in the paper. In Section III, the problem of continuous time trajectory planning with risk bounds is formulated. In section IV, An analytical approach is provided to compute, for static and dynamic obstacles, risk boundaries to define zones of safe operation in uncertain environments. We present in Section V techniques for tracing irregular and continuously time-bounded trajectories in uncertain dynamic and static environments using sum-of-squares. Section VI presents applications related to the risk bounded planning problems that arise in autonomous and robotic systems. The final section concludes the work with some thoughts about future work.

2. Notation and Preliminaries

The polynomials, moments of probability distributions, the sum of squares optimization are described here with definitions and notations. Given a vector $x \in \mathbb{R}^n$ and multiindex $\alpha \in \mathbb{N}^n$, let $x^\alpha = \prod_{i=1}^n x_i^{\alpha_i}$.

Polynomial Expression: Let the set of all real polynomials in the variables $x \in \mathbb{R}^n$ be $\mathbb{R}[x]$ given polynomial $\mathcal{P}(x) : \mathbb{R}^n \rightarrow \mathbb{R}$, we denoted \mathcal{P} as $\sum_{\alpha \in \mathbb{N}^n} p_\alpha x^\alpha$ where $\{x^\alpha\}_{\alpha \in \mathbb{N}^n}$ are standard monomial basis of the $\mathbb{R}[x]$, $\mathcal{P} = \{p_\alpha\}_{\alpha \in \mathbb{N}^n}$ expressing the coefficients, and $\alpha \in \mathbb{N}^n$. The paper describes continuous-time trajectories and uncertain obstacles using polynomials.

Moments of Probability Distributions: It is defined as the expected value of a monomial of random variables. Random variables constitute the generalization of means and co-variances. Specifically, given $(\alpha_1, \alpha_2, \dots, \alpha_n) \in \mathbb{N}^n$ where $\alpha = \sum_{i=1}^n \alpha_i$, moments of order α of random vector η is defined as $\mathbb{E}[\prod_{i=1}^n \eta_i^{\alpha_i}]$. A sequence of the moments for $n = 3$ of order $\alpha = 2$ has the following definition $\mathbb{E}[\eta_1^2]$, $\mathbb{E}[\eta_1 \eta_2]$, $\mathbb{E}[\eta_1 \eta_3]$, $\mathbb{E}[\eta_2^2]$, $\mathbb{E}[\eta_2 \eta_3]$, $\mathbb{E}[\eta_3^2]$. A probability distribution’s characteristic function [19] can be used to calculate the moments of random variables. In order to represent non-Gaussian probability distributions, a finite sequence of moments will be used.

Sum of Squares (SOS) Polynomials and Optimization: SOS techniques are used in this paper to solve nonconvex optimization problems involving risk-bounded trajectory planning. If the any polynomial $\mathcal{P}(x)$ can be defined as a sum of finitely many squares, then the polynomial is named as a sum of squares polynomial. i.e., $\mathcal{P}(x) = \sum_{j=1}^m f_j(x)^2$ for all $m < \infty$ & $f_j(x) \in \mathbb{R}[x]$ for $1 \leq j \leq m$. The linear matrix inequality (LMI) can be represented by the coefficients of the polynomial in the SOS condition, that is, $\mathcal{P}(x) \in \text{SOS} \rightarrow \mathcal{P}(x) = x^T A x$ where A is the positive semi-definite matrix in which obtain from coefficients of the polynomials [20–22], and x is the vector of the standard monomial basis. There are multiple software packages available that can be used to test SOS condition of polynomials like Yalmip [23] and Spotless [24]. Convex relaxations are obtained by using sum of squares polynomials for nonconvex polynomial optimization problems [20–22]. Recently, SOS optimization techniques have been used to prove the time-varying polynomials optimization problems of the following type

$$\begin{aligned} & \min_{x \in \mathbb{R}^n} f(x) \\ & \text{subject to } g_i(t, x) \geq 0, \text{ for all } t \in [t_0, t_f], i = 1, 2, \dots \end{aligned} \tag{1}$$

The given time horizon $t \in [t_0, t_f]$ should be checked to see that time-varying constraints are satisfied. SOS-based techniques can solve the time-varying optimization problem in (1) by transforming it into a convex optimization, i.e., a semidefinite program [25, 26]. In this paper, we provide SOS optimizations to construct risk contours.

3. Problem Formulation

Let $\psi_{obs_i}(\eta_i)$ be a static uncertain obstacle defined in terms of polynomial \mathcal{P}_i as follows [3]

$$\psi_{obs_i}(\eta_i) = \{x \in \psi : \mathcal{P}_i(x, \eta_i) \geq 0\}, i = 1, 2, \dots, n_{o_s} \tag{2}$$

where, $\psi \subset \mathbb{R}^n$ is a uncertain environment, $\eta_i \in \Omega \subset \mathbb{R}^m$ these parameters have known probability distributions and are probabilistic uncertain parameters $\mathcal{P}_i : \mathbb{R}^{n_s+n_\eta} \rightarrow \mathbb{R}$ are given polynomial in $x \in \psi$ and $\eta_i \in \Omega$. Similarly, we represent $\psi_{obs_i}(\eta_i, t)$ are describe an uncertain dynamic obstacle as a polynomial \mathcal{P}_i , time t and probabilistic uncertain parameters with known probability distributions as follows

$$\psi_{obs_i}(\eta_i, t) = \{x \in \psi : \mathcal{P}_i(x, \eta_i, t) \geq 0\}, i = n_{o_s} + 1, \dots, n_{o_d} \tag{3}$$

where $\mathcal{P}_i : \mathbb{R}^{n_s+n_\eta+1} \rightarrow \mathbb{R}$ are given polynomial. Note that, the sets (2) and (3) represents an nonconvex obstacle with probabilistic, e.g., obstacle with uncertain size, location, or geometry [3, 27]. In general, we can represent uncertain safe region as follows

$$\psi_{safe}(\eta) = \psi - \psi_{obs}(\eta) \tag{4}$$

According to our definition of risk, this is dependent on the agent's size and ego vehicle. An agent is supposed to be fit with director circles of an ellipse of radius using a collision ellipsoid around the vehicle, and the probability that the centers of the director circles fall within that ellipsoid must be limited. The Figure 1 illustrates how the director circle of an ellipse circumscribes its minimum bounding box. The ellipse and its director circle share the same center and radius $\sqrt{\eta_1^2 + \eta_2^2}$ where η_1 and η_2 are semimajor axis and semiminor axis make up the ellipse respectively.

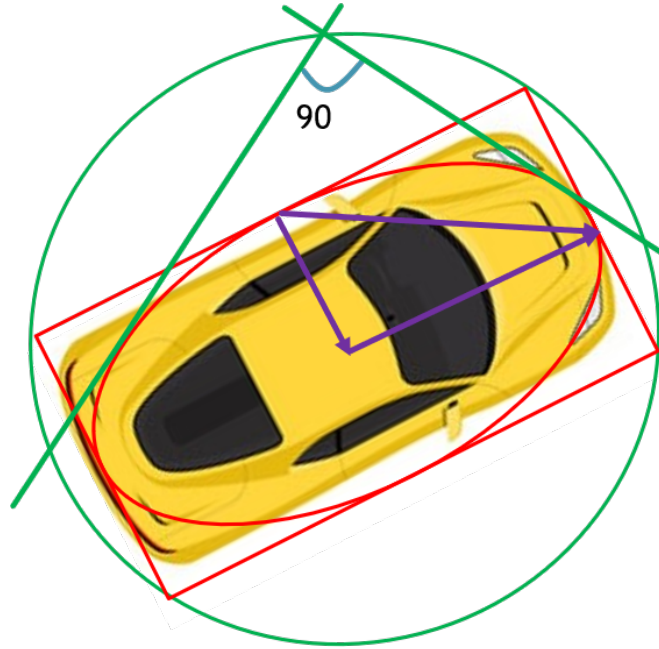


Figure 1: A director circle, an ellipse, and its minimum bounding box

The probability of colliding with something is defined as risk with uncertain obstacles in the environment given static and dynamic uncertainties in (2) and (3). With the goal of determining a continuous-time trajectory within a risk envelope, we consider the risk-bounded continuous-time trajectory planning problem $x(t) : [t_0, t_f] \rightarrow \mathbb{R}^{n_x}$ denoted over in the time interval $t \in [t_0, t_f]$ from the points start to the finish x_0 and x_f , the trajectory $x(t)$ is so designed that the colliding with uncertain obstacles is inner bounded. As a result, we arrive at the following probabilistic optimization problem for continuous time trajectory planning:

$$\min_{x(t): [t_0, t_f] \rightarrow \mathbb{R}^{n_x}} \int_{t_0}^{t_f} \|\dot{x}(t)\| dt \quad (5a)$$

$$\text{subject to } x(t_0) = x_0, \quad x(t_f) = x_f$$

$$\text{Prob}(x(t) \in \Psi_{obs_i}(\eta_i)) \leq \Delta \quad (5b)$$

$$\text{Prob}(x(t) \in \Psi_{obs_i}(\eta_i, t)) \leq \Delta \quad (5c)$$

where $x(t)$ is the trajectory length in the objective function (5) which denoted in the ℓ_2 norm. Furthermore, the constraints (5b) and (5c) are defined as the static and dynamic obstacles that present a risk at time t for trajectory $x(t)$. We've determined that $0 \leq \Delta \in \mathbb{R} \leq 1$ is the risk level to be accepted.

We will use piecewise linear trajectories of the form (5) to solve the risk-bounded optimization problem

$$x_i(t) = a_i + b_i t, \quad t \in [t_{i-1}, t_i], \quad i = 1, 2, 3, \dots, s \quad (6)$$

Each linear piece is defined over a given time interval and is given a number s , here $t \in [t_{i-1}, t_i]$ in the form of $t_{i-1} = t_0 + \frac{(i-1)(t_f - t_0)}{s}$ and $t_i = t_0 + \frac{i(t_f - t_0)}{s}$, $a_i, b_i \in \mathbb{R}^{n_x}$ the coefficient vectors.

4. Risk Contours

Here, we suggest an optimization-free fast approach, referred to as an analytical approach, we present a method for constructing risk region for the static and moving obstacles and illustrate how the contours can be used for risk-bounded trajectory planning (5).

4.1. Static Risk Contours

Let $\Psi_{obs}(\eta) = \{x \in \Psi : \mathcal{P}(x, \eta) \geq 0\}$, the static or no-moving uncertain obstacle is described as follows (2) and Δ between $[0, 1]$, this is the level of risk that is acceptable. The risk contour of given Δ is determined by \mathcal{C}_r^Δ and it is in set of all points in the environment, that is, $x \in \Psi$, the risk is less than or equal to Δ . In order to be more precise,

$$\mathcal{C}_r^\Delta = \{x \in \Psi : \text{Prob}(x(t) \in \Psi_{obs}(\eta)) \leq \Delta\} \quad (7)$$

For (7) to produce the static risk contour, the probabilistic constraint must be replaced by a static one, that is to say $\text{Prob}(x(t) \in \psi_{obs}(\eta)) = \text{Prob}(\mathcal{P}(x, \eta) \geq 0) \leq \Delta$, in terms of x , there is a deterministic constraint. In this paper, we propose the following analytical method; The polynomial that describes the upper bound of the collision probability can be denoted by $\mathcal{P}(x, \eta)$ for the uncertain obstacle $\psi_{obs}(\eta)$, we define the set \mathcal{C}_r^Δ as follows

$$\mathcal{C}_r^\Delta = \left\{ x \in \Psi : \frac{\text{Var}[\mathcal{P}(x, \eta)]}{\text{Var}[\mathcal{P}(x, \eta)] + \mathbb{E}[\mathcal{P}(x, \eta)]^2} \leq \Delta, \mathbb{E}[\mathcal{P}(x, \eta)] \leq 0 \right\} \tag{8}$$

with respect to the uncertainty parameter η , the expectation of a parameter is taken. There are polynomials that can be computed $\mathbb{E}[\mathcal{P}^2(x, \eta)]$ and $\mathbb{E}[\mathcal{P}(x, \eta)]$, with known moment of η is given as x .

The set \mathcal{C}_r^Δ in (8) is an inner approximation of the static risk contour \mathcal{C}_r^Δ in (7). The theorem 4.1 can be easily proved as proved in [10], Hence we omitted the proof here. We refer to the reader to read similar proof given in [10] for understanding.

The inner approximation of the function \mathcal{C}_r^Δ is \mathcal{C}_r^Δ , so any trajectory $x(t) \in \mathcal{C}_r^\Delta$ that has all $t \in [t_0, t_f]$ has a guarantee that the risk is less than or equal Δ . Here we provide an example to illustrate how the proposed method converts static risk contours into Δ -risk contours.

Remark: It is possible to extend the method proposed in this paper to more complex sets that involve multiple polynomials, even though unsafe obstacles are defined by just one polynomial. The assumptions in this section are only for the purpose of simplifying the exposition.

Example A. The following is an example of an illustrative scenario $\psi = [-1, 1]^2$. The set $\psi_{obs}(\eta) = \{(x_1, x_2) : \eta_1^2 + \eta_2^2 - x_1^2 - x_2^2 \geq 0\}$ the obstacle has the shape of a director circle, whose radius is measured $\sqrt{\eta_1^2 + \eta_2^2}$ it is composed of an uniform probability distribution in the range [0.3, 0.4] and a normal probability distribution in the range [0, 0.1].

A uniform distribution defined over $[l, u]$ has a moment of α order, normal distribution describe over $[\mu, \sigma]$ can be described in a closed-form as $y_\alpha = \frac{u^{\alpha+1} - l^{\alpha+1}}{(u-l)(\alpha+1)}$ and $y_\alpha = \sigma^\alpha (-\sqrt{-1}\sqrt{2})^\alpha \text{kummerU}(\frac{-\alpha}{2}, \frac{1}{2}, \frac{-\mu^2}{2\sigma^2})$, respectively, where kummerU is confluent hyper-geometric KummerU function.

In order to develop the static Δ risk contour region, we find the polynomials' $\mathbb{E}[\mathcal{P}(x, \eta)]$, and $\mathbb{E}[\mathcal{P}^2(x, \eta)]$ out of the polynomial obstacles and η moments as given as follows:

$$\begin{aligned} \mathbb{E}[\mathcal{P}(x, \eta)] &= \mathbb{E}[\eta_1^2 + \eta_2^2 - x_1^2 - x_2^2] = 0.1333 - x_1^2 - x_2^2 \\ \mathbb{E}[\mathcal{P}^2(x, \eta)] &= \mathbb{E}[(\eta_1^2 + \eta_2^2 - x_1^2 - x_2^2)^2] \\ &= x_1^4 + 2x_1^2x_2^2 - (4x_1^2)/15 + x_2^4 - (4x_2^2)/15 + 0.0184. \end{aligned}$$

As shown in Figure 2, we use sub levels of functions as in (8) to construct the inner approximation of the static Δ -risk contour map for the different levels of risk are $\Delta = [0.01, 0.03, 0.5]$. Outside of the circles represents inner approximations of Δ -risk contours. If agents or vehicle are enter cross the 0.5 lane then there is a 50% of possibility of collision (risk), if cross the 0.03 lane then there is a 3% of possibility of collision, if cross the 0.01 lane then there is a 1% of possibility of collision. We describe the uncertain obstacle in the blue line.

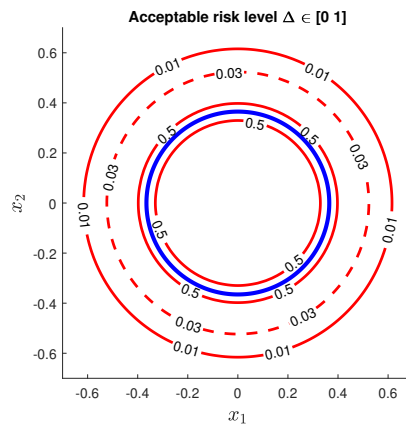


Figure 2: Static Δ -risk contours as described in (8).

4.2. Dynamic Risk Contours

Let $\psi_{obs}(t, \eta) = \{x \in \Psi : \mathcal{P}(t, \eta, x) \geq 0\}$, the dynamic or moving uncertain obstacle is expressed as follows (3) and Δ between $[0, 1]$ this is the level of risk that is acceptable. The risk contour Δ is determined by \mathcal{C}_r^Δ , and the set of all points in the environment, that is, $x \in \Psi$, whose risk is less than or equal to Δ . In order to be more precise,

$$\mathcal{C}_r^\Delta(t) = \{x \in \Psi : \text{Prob}(x(t) \in \psi_{obs}(\eta, t)) \leq \Delta\} \tag{9}$$

Constructing a dynamic risk contour in this way is the important concept in (9), the probabilistic constraints will be replaced, which means we can say that

$$\text{Prob}(x(t) \in \psi_{obs}(\eta, t)) = \text{Prob}(\mathcal{P}(x, \eta, t) \geq 0) \leq \Delta,$$

with a deterministic constraint in terms of x . As a result of this paper, we propose the following analytical method:

The polynomial can be used to describe the upper bound of the probability of collision $\mathcal{P}(x, \eta, t)$ of the uncertain obstacle $\psi_{obs}(\eta, t)$, Definition of the set $\hat{\mathcal{C}}_r^\Delta(t)$ as follows

$$\hat{\mathcal{C}}_r^\Delta(t) = \left\{ x \in \Psi : \frac{\text{Var}[\mathcal{P}(x, \eta, t)]}{\text{Var}[\mathcal{P}(x, \eta, t)] + \mathbb{E}[\mathcal{P}(x, \eta, t)]^2} \leq \Delta, \right. \\ \left. \mathbb{E}[\mathcal{P}(x, \eta, t)] \leq 0 \right. \quad (10)$$

In terms of the time-varying constraints, dynamic Δ -risk contour (10) has been described.

Example B. The following is an example of an illustrative scenario $\Psi = [-1, 1]^2$. The set $\psi_{obs}(\eta) = \{(x_1, x_2) : \eta_1^2 + \eta_2^2 - (x_1 - p_{x_1}(t, \eta_3))^2 - (x_2 - p_{x_2}(t, \eta_4))^2 \geq 0\}$ denotes a director circle structure obstacle whose radius is $\sqrt{\eta_1^2 + \eta_2^2}$ and uncertain trajectories $p_{x_1}(t, \eta_3) = t^2 + 1 - 4t + 0.2\eta_3$, $p_{x_2}(t, \eta_4) = t^2 - 1 + 3t + 0.1\eta_4$ that describe time horizon $t \in [0, 1]$, over which the obstacle moves uncertainly. Uncertain parameters have uniform, normal, beta, and gamma distribution as $\eta_1 \sim \text{Uniform}[0.3, 0.4]$, $\eta_2 \sim \text{Normal}[0, 0.1]$, $\eta_3 \sim \text{Beta}[3, 3]$, $\eta_4 \sim \text{Gamma}[0.2, 0.8]$.

Beta- and Gamma-distribution moment of order α , with parameters (a, b) can be give in the closed-forms as $y_\alpha = \frac{a+\alpha-1}{a+b+\alpha-1}y_{\alpha-1}$, $y_0 = 1$, and $y_\alpha = b(a+\alpha-1)y_{\alpha-1}$, $y_0 = 1$, respectively. Same as illustrative example A, we can find the nonnegative polynomials $\mathbb{E}[\mathcal{P}(x, \eta, t)]$ and $\mathbb{E}[\mathcal{P}^2(t, \eta, x)]$ using the moment of uncertain parameters $\eta_i, i = 1(1)4$ and the obstacle of the polynomial. Based on the dynamic Δ -risk contour, as defined by (10), we developed the dynamic or moving Δ -risk profile of function of time.

Figure 3 shows, the calculated moving Δ -risk contours with time $t = 0, 0.5, 1$ for $\Delta = 0.1$ along with a uncertain trajectory $(p_{x_1}(t, \eta_3), p_{x_2}(t, \eta_4))$ are obtained. An uncertain trajectory is represented by a dashed path that shows its expected value. For any point inside $\hat{\mathcal{C}}_r^\Delta(t)$ at time t , in uncertain moving obstacles, $\Delta = 0.1$ is less or equal to the probability of collision.

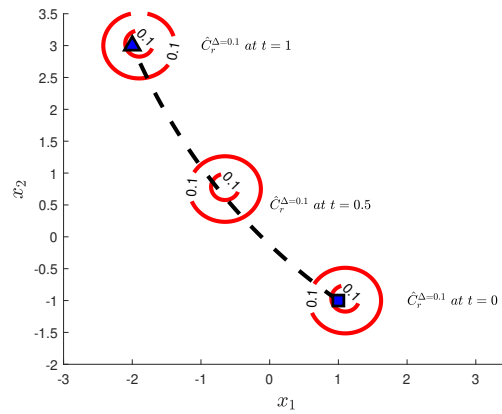


Figure 3: Dynamic Δ -risk contours as described in (10).

Remark: In real-time, we can construct static and dynamic risk contours using (8) and (10). For this reason, standard motion planning algorithms can be used for real-time risk assessment, such as PRM, RRT* and motion primitive-based methods such as "bounded motion planning". It is easy to accomplish this by using the risk contours, i.e., safe regions, when constructing the trajectory.

5. Planning using risk contours in uncertain static and dynamic environments

5.1. Planning in static uncertain environments

Suppose there are static uncertain obstacles of the form (2) on the trajectory. Then continuous time bounded trajectory planning applies. Specifically, in (5), we are attempting to solve the probability optimization problem when uncertain obstacles are present $\psi_{obs_i}(\eta_i), i = 1, 2, \dots$. As a result of replacing the probabilistic constraints (5)b with deterministic constraints of the static Δ -risk contours, the deterministic polynomial optimization can be obtained as follows:

$$\min_{x(t): [t_0, t_f] \rightarrow \mathbb{R}^{n_x}} \int_{t_0}^{t_f} \|\dot{p}(t)\| dt \quad (11a)$$

$$\text{subject to } x(t_0) = x_0, \quad x(t_f) = x_f$$

$$x(t) \in \hat{\mathcal{C}}_{r_i}^\Delta, \quad t \in [t_0, t_f], \quad i = 1, 2, \dots, n_{o_s} \quad (11b)$$

here $\hat{\mathcal{C}}_{r_i}^\Delta$ is the static risk contour of the uncertain obstacle $\psi_{obs_i}(\eta_i)$.

A deterministic optimization in (11) can only be achieved if all constraints are satisfied over the entire planning time horizon $[t_0, t_f]$. To solve the deterministic optimization problem in (11), we will use the piecewise linear trajectory defined in (6). We must guarantee that we satisfy the constraints over the entire planning time horizon $[t_0, t_f]$ in order to obtain deterministic optimization in (11). We will use piecewise linear trajectory defined in (6) to solve the deterministic optimization problem in (11). In an implementation, deterministic polynomial optimization is solved using time-varying SOS optimization. The algorithm for this was introduced in [26].

Example C. In illustrative example A, we see an uncertain obstacle. The deterministic optimization problem (11) is solved to get linear trajectories with piece-wise using the time varying SOS optimizations with the Δ -risk contours of uncertain obstacles, like in Figure 4 the 0.1-risk contour corresponds to the intersection of $x(0) = [1, -1]$ and $x(1) = [-1, 1]$.

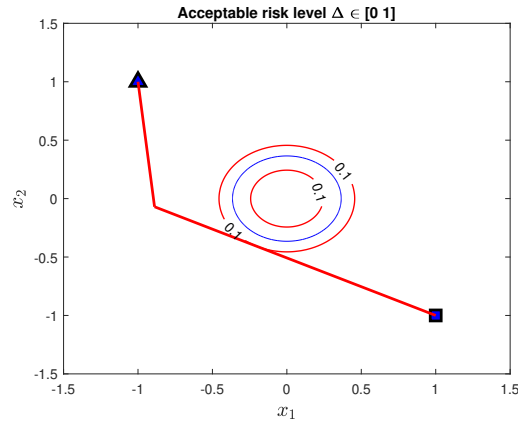


Figure 4: Time-varying SOS optimization with a probability-based static obstacle yields a piece-wise linear trajectory bound by risk.

5.2. Planning in Dynamic Uncertain Environments

Under dynamic or moving uncertain obstacles of the form as given in (3), we take a look at continuous-time risk-bounded trajectory planning. When faced with dynamic uncertainties $\psi_{obs_i}(\eta_i, t), i = 1, 2, \dots$, we aim to solve the optimization problem in (5). Using the static Δ -risk contours as deterministic constraints (5)c, we can obtain the deterministic polynomial optimization

$$\min_{x(t): [t_0, t_f] \rightarrow \mathbb{R}^{n_x}} \int_{t_0}^{t_f} \|\dot{p}(t)\| dt \tag{12a}$$

subject to $x(t_0) = x_0, x(t_f) = x_f$

$$x(t) \in \mathcal{C}_{r_i}^\Delta, t \in [t_0, t_f], i = n_{os} + 1, \dots, n_{od} \tag{12b}$$

here $\mathcal{C}_{r_i}^\Delta$ is the moving 0.1-risk contour of the motion uncertain obstacle $\psi_{obs_i}(\eta_i, t)$. In (12) we obtain deterministic optimization by stating the constraints and ensuring to satisfy them throughout the entire planning horizon $[t_0, t_f]$. Using the time-varying SOS optimization described in the previous section, we will solve the time-varying deterministic polynomial optimization in (12).

Example D. Take example B as an example of a moving obstacle. Optimizing the SOS with time-varying parameters, we wish to derive piece wise trajectories within Δ -risk of the uncertain moving obstacles between the given bounded region points $x(0) = [1, -2]$ and $x(1) = [1, 3]$ using a deterministic optimization problem in (12). In Figure 5, we apply the time-varying SOS optimization algorithm to solve the deterministic optimization problem in (12) when used with regard to the dynamic 0.1-risk contour of the uncertain obstacle. An uncertain moving obstacle trajectory is represented by a dashed path. An uncertain moving agent vehicle trajectory is represented by a solid blue line.

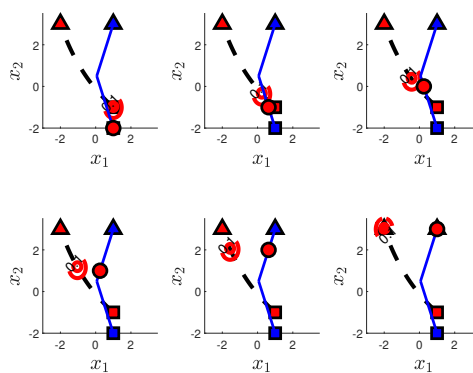


Figure 5: Time-varying SOS optimization with the probabilistic moving obstacle yields a piece-wise linear trajectory subject to risk.

6. Application

6.1. Autonomous vehicle lane changing in a risk-bound manner

In this application, an autonomous vehicle is shown to change lanes in the presence of surrounding vehicles, with an adapted risk bounded trajectory. The following sets of models are used to model the uncertain locations of surrounding vehicles in this scenario $\psi_{obs_1}(\eta_1, t) = \{(x_1, x_2) : \eta_1^2 + \eta_2^2 - (x_1 - p_1(t, \eta_1))^2 - x_2^2 \geq 0\}$ and $\psi_{obs_2}(\eta_2, t) = \{(x_1, x_2) : \eta_1^2 + \eta_2^2 - (x_1 - p_2(t, \eta_1))^2 - (x_2 - 1)^2 \geq 0\}$ where $p_1(t, \eta_1) = t + 0.4 + \eta_1$ and $p_2(t, \eta_1) = 2t + 0.6 + \eta_1$ are the uncertain trajectories of the surrounding vehicles with uncertain

parameters have uniform, normal distribution as $\eta_1 \sim \text{Uniform}[-0.1, 0.1]$, $\eta_2 \sim \text{Normal}[0, 0.1]$. Over the planning time horizon $t \in [0, 1]$, we seek a lane-change maneuver trajectory that is risk bound between the points $x(0) = [0, 0]$ and $x(1) = [2, 1]$. Based on the 0.1-risk contours of the surrounding vehicles within the dynamic 0.1-risk trajectory, Figure 6 shows the obtained trajectory. An uncertain moving obstacle trajectory is represented by a dashed path that shows its expected value. Risk-bound lane-change trajectories between start (square) and goal (triangle) points in the presence of uncertain surrounding trajectories, as determined from the time-varying SOS optimization proposed in this work (red dotted line) and proposed in [10] (green dotted line) and RRT-SOS (blue solid line).

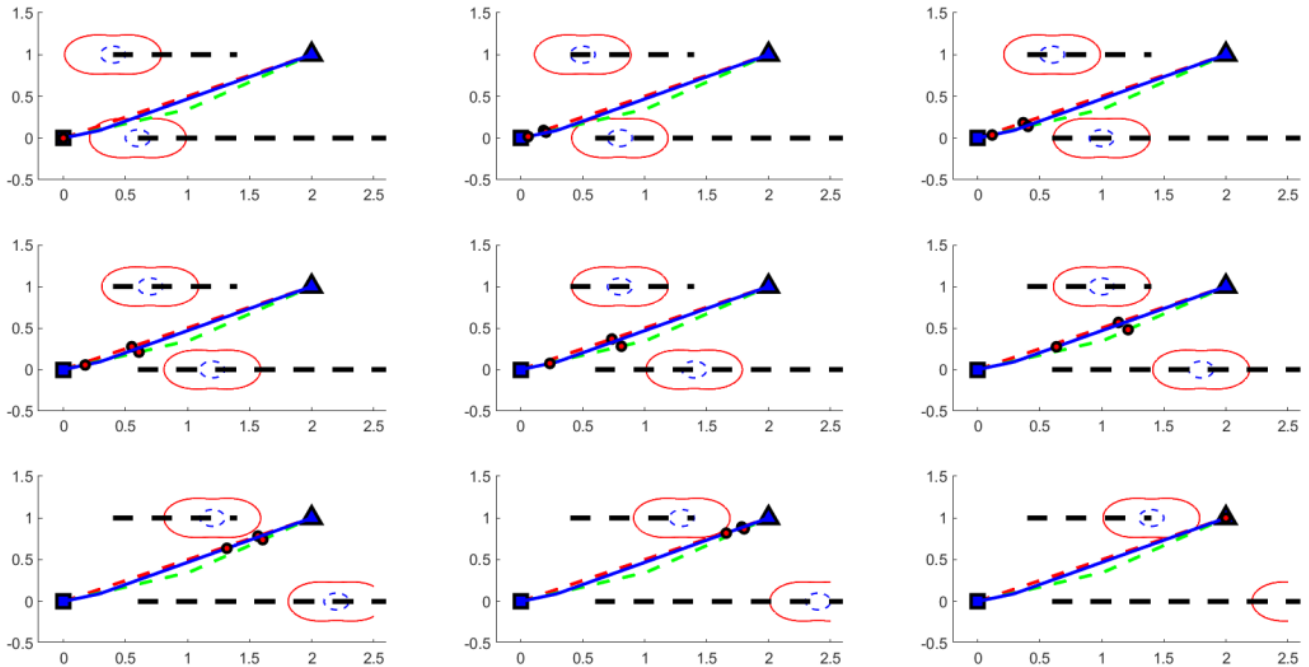


Figure 6: Risk-bound lane-change trajectories for Autonomous vehicle

7. Conclusion

We have presented continuous-time trajectory planning algorithms that generate risk-bounded polynomial trajectories in uncertain nonconvex environments where obstacles are distributed over space with probabilistic locations, sizes, and shapes. Convex methods are employed to obtain continuous-time trajectories with guaranteed bounded risk without time discretization by leveraging the notion of risk contours and transforming the probability-based trajectory planning problem into a deterministic planning problem. A model predictive control (MPC) framework will be developed in the future to handle the online planning problems.

References

- [1] J. Reif and M. Sharir. Motion planning in the presence of moving obstacles. *Journal of the ACM*, 41(4):764–490, 1994.
- [2] L. Blackmore, H. Li, and B. C. Williams. A probabilistic approach to optimal robust path planning with obstacles. *American Control Conference (ACC), Minneapolis*, 2006.
- [3] A. Jasour, A. Hofmann, and B.C. Williams. Moment-sum-of-squares approach for fast risk estimation in uncertain environments. *IEEE Conference on Decision and Control (CDC), Florida, USA*, 2018.
- [4] M. Ono L. Blackmore. Convex chance constrained predictive control without sampling. *AIAA Guidance, Navigation, and Control Conference, Chicago*, 2009.
- [5] W. Liu and M. H. Ang. Incremental sampling-based algorithm for risk-aware planning under motion uncertainty. *IEEE International Conference on Robotics and Automation (ICRA), Hong Kong*, 2014.
- [6] L. Janson, E. Schmerling, and M. Pavone. Monte carlo motion planning for robot trajectory optimization under uncertainty. *Springer Proceedings in Advance Robotics Book Series 3, Robotics Research*, 2:343–361, 2018.
- [7] E. Schmerling and M. Pavone. Evaluating trajectory collision probability through adaptive importance sampling for safe motion planning. *Robotics: Science and Systems (RSS), MIT*, 2017.
- [8] M. Ono and B. C. Williams. Iterative risk allocation: A new approach to robust model predictive control with a joint chance constraint. *IEEE Conference on Decision and Control (CDC), Cancun, Mexico*, 2008.
- [9] A. Pierson, W. Schwarting, S. Karaman, and D. Rus. Navigating congested environments with risk level sets. *IEEE International Conference on Robotics and Automation (ICRA), Australia*, 2018.

- [10] Ashkan Jasour, Weiqiao Han, and Brian Williams. Convex risk bounded continuous-time trajectory planning in uncertain nonconvex environments. 2021. URL <https://arxiv.org/abs/2106.05489>.
- [11] A. Jasour, N. S. Aybat, and C. Lagoa. Semidefinite programming for chance constrained optimization over semialgebraic sets. *SIAM Journal on Optimization*, 25(3):1411–1440, 2015.
- [12] A. Jasour. Convex approximation of chance constrained problems: Application in systems and control. *School of Electrical Engineering and Computer Science, The Pennsylvania State University*, 2017.
- [13] A. A. Ahmadi, G. Hall, A. Makadia, and V. Sindhvani. Geometry of 3d environments and sum of squares polynomials. *Robotics: Science and Systems (RSS), MIT*, 2017.
- [14] A. Majumdar, A. A. Ahmadi, and R. Tedrake. Control design along trajectories via sum of squares optimization. *International Conference on Robotics and Automation (ICRA), MN, USA*, 2012.
- [15] S. Shen and R. Tedrake. Compositional verification of large-scale nonlinear systems via sums-of-squares optimization. *American Control Conference (ACC), Milwaukee, USA*, 2018.
- [16] M. Posa, T. Koolen, and R. Tedrake. Balancing and step recovery capturability via sums-of-squares optimization. *Robotics: Science and Systems, MIT*, 2017.
- [17] R. Tedrake, I R. Manchester, M. M. Tobenkin, and J. W. Roberts. Lqr-trees: Feedback motion planning via sums of squares verification. *International Journal of Robotics Research*, 29(July):1038–1052, 2010.
- [18] A. Majumdar and R. Tedrake. Funnel libraries for real-time robust feedback motion planning. *International Journal of Robotics Research*, 36(8):947–982, 2017.
- [19] J. Jacod and P. Protter. Probability essentials. *Springer Science & Business Media*, 2012.
- [20] P. A. Parrilo. Semidefinite programming relaxations for semialgebraic problems. *Mathematical programming*, 96(2), 2003.
- [21] J. B. Lasserre. Global optimization with polynomials and the problem of moments. *SIAM Journal on optimization*, 11(2):796–817, 2001.
- [22] M. Laurent. Sums of squares, moment matrices and optimization over polynomials. *Emerging Applications of Algebraic Geometry, Springer*, pages 157–270, 2009.
- [23] J. Lofberg. Yalmip: A toolbox for modeling and optimization in matlab. *IEEE International Conference on Robotics and Automation (ICRA)*, 2004.
- [24] M. M. Tobenkin, F. Permenter, and A. Megretski. spotless: Polynomial and conic optimization. *IEEE International Conference on Robotics and Automation (ICRA)*, 2013. URL [\[Online\]. Available:github.com/spot-toolbox/spotless](https://github.com/spot-toolbox/spotless).
- [25] A. A. Ahmadi and B. E. Khadir. Time-varying semidefinite programs,” mathematics of operations research. *arXiv:1808.03994*, 2021.
- [26] B. E. Khadir, J. B. Lasserre, and V. Sindhvani. Piecewise-linear motion planning amidst static, moving, or morphing obstacles. *IEEE International Conference on Robotics and Automation (ICRA)*, 2021.
- [27] A. Jasour and B. Williams. Risk contours map for risk bounded motion planning under perception uncertainties. *Robotics: Science and Systems*, 2019.